J Solid State Electrochem (2009) 13:843–847
DOI 10.1007/s10008-008-0621-4

ORIGINAL PAPER

Electrodeposited magnetite with large magnetoresistive response at room temperature and low magnetic fields

R. G. Delatorre · R. C. da Silva · J. S. Cruz · N. Garcia · A. A. Pasa

Received: 24 April 2008 / Revised: 19 June 2008 / Accepted: 24 June 2008 / Published online: 12 July 2008

Abstract Iron oxide layers were obtained by electrodeposition method on Cu substrates. The electrolyte containing $Fe_2(SO_4)_3$, NaOH, and Triethanolamine was stirred at a temperature of 65 °C and the depositions were performed potentiostatically in a conventional three electrode cell at a potential of −1.1 V vs SCE. Parallel magnetoresistance values of −6.2% at 3 kOe were obtained for measurements at room temperature. The magnetoresistive curves showed reduced hysteresis loop, temporal stability, and no saturation for the maximum applied magnetic field. Our results show that for the case of the granular magnetite that we grow, the AMR has opposite sign of that of 3d magnetic alloys. Allied to high values of resistivity, these properties are potentially adequate for the development of magnetic devices such as field sensors. Additional characterization was obtained by using scanning electron microscopy and vibrating sample magnetometry.

Introduction

The preparation of iron oxide layers with composition close to the magnetite phase (Fe_3O_4) have been investigated with techniques such as sputtering [1–3], molecular beam epitaxy [4], laser ablation [5, 6], electroless plating [7, 8], and electrodeposition [9, 10]. Magnetite is an important iron oxide phase, a half-metallic ferromagnet [11], potentially considered for the development of spintronic devices and magnetic field sensors. In other words, the nowadays interesting property of magnetite is the magnetotransport due to strong spin polarization at the Fermi level. Coey and coauthors investigated the magnetoresistance (MR) of magnetite in the form of polycrystalline thin film, powder compact, and single-crystal, measuring room temperature values as high as −1.6% at 0.5 T [12]. The results were explained assuming the alignment of the magnetization of contiguous grains by the applied field. Eerenstein et al. [4] studied the spin-polarized transport across magnetite boundaries grown epitaxially on MgO, observing a magnetoresistive behavior that was described by the hopping model, with spin-polarized electrons crossing an antiferromagnetic interface separating two ferromagnetic domains, known as antiphase boundaries [13, 14]. More recently, magnetite nanoparticle systems have presented high values of magnetoresistance at room temperature, however, for very high applied magnetic fields, i.e., −12% at 35 kOe [15] and −22.8% at 150 kOe [16].

In this work, we will present the magnetoresistance of electrodeposited iron oxide with composition close to the magnetite phase. Magnetoresistive values of −6.2% at 3 kOe and room temperature were obtained. In the literature, comparable MR values for magnetite were reported for electroless plated films [7], nanowires electroprecipitated in templates [9], and rf sputtering deposited ultrathin films [17].

Experimental procedure

The substrates used in our experiments were printed circuit boards (PCBs), which are composed of a laminated copper

R. G. Delatorre · N. Garcia · A. A. Pasa (✉)
Laboratorio de Fisica de Sistemas Pequeños y Nanotecnología,
CSIC,
Calle Serrano 144,
28006 Madrid, Spain
e-mail: pasa@fisica.ufsc.br

R. C. da Silva · J. S. Cruz · A. A. Pasa
Laboratório de Filmes Finos e Superfícies, UFSC,
CP 476,
88.040-900 Florianópolis, Brazil

sheet onto a nonconductive substrate. Each substrate with size of about 1×2 cm was cleaned with a solution containing 0.2 M HNO_3, to remove copper oxide from the surface, and immersed in the electrodeposition cell. All the electrolytes, as well as etching solutions used to clean the samples prior to the electrochemical experiments, were prepared from filtered deionized water with a resistivity of 18 MOhm cm and analytical grade reagents. The electrochemical experiments were performed in a conventional three-electrode cell. The potentials were measured against a saturated calomel electrode (SCE) which was placed as close as possible to the Cu surface to minimize the ohmic potential drop in the electrolyte. The Pt foil counter electrode was placed directly opposite the working electrode (substrate). The magnetite deposits on Cu were prepared from an aqueous electrolyte analogous to the one used in [10], with different concentration of the reagents, i.e., 45 mM of $Fe_2(SO_4)_3$, 76 mM of NaOH, and 37 mM of Triethanolamine (TEA). All electrochemical experiments were performed by stirring the electrolyte at 65 °C, and electrodeposits at an applied potential of −1.1 V vs. SCE.

The samples were characterized by electrical and magnetoresistive measurements using a dc two-probe method. Due to the fact that the substrate is conductive, acting as one terminal, the second terminal was simple, a copper wire connected to the surface with silver paste. For the magnetoresistive measurements, the magnetic field was applied parallel and perpendicular to the electric current, which is perpendicular to the sample surface, with intensity varying in the range of 0 to 3 kOe. The magnetoresistance effect was calculated using the equation MR (%)=100[R_m−R_0]/R_0, where R_m is electrical resistance at the maximum applied field, and R_0 is maximum value of the resistance at low magnetic fields. Additional characterization was obtained using scanning electron microscopy (SEM-Philips XL30) with field emission gun and energy dispersive spectroscopy (EDS), and vibrating sample magnetometry (VSM-Model 9500, LDJ Electronics, Inc.).

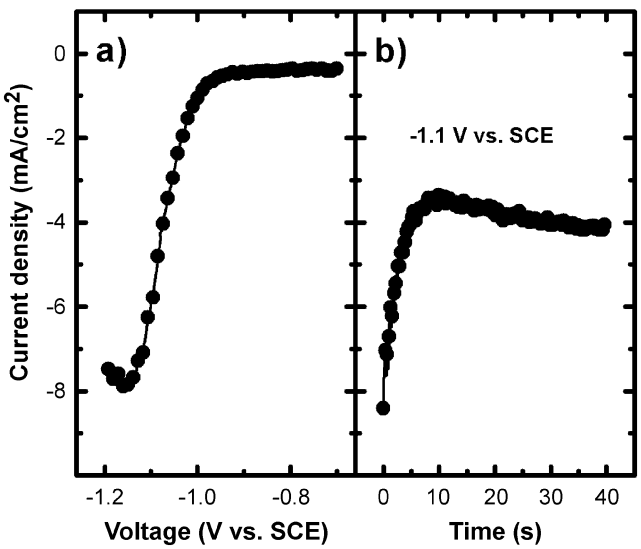

Fig. 1 **a** Polarization curve and **b** current transient obtained on the surface of Cu working electrode (PCB substrates) at 65 °C with an electrolyte containing 45 mM of $Fe_2(SO_4)_3$, 76 mM of NaOH, and 37 mM of Triethanolamine (TEA)

Results and discussion

Figure 1a displays a typical polarization curve obtained on Cu surfaces (PCB substrates) with potential scan rate of 10 mV/s. The reduction starts at about −0.95 V and reaches a peak at −1.15 V. This polarization curve is similar to the cyclic voltammogram presented in [10], where the authors describe the cathodic behavior by the two-step reduction reaction that lead to the formation of magnetite shown in Eqs. 1 and 2:

$$Fe(TEA)^{3+} + e^- \rightarrow Fe^{2+} + TEA, \quad (1)$$

and

$$Fe^{2+} + 2Fe(TEA)^{3+} + 80H^- \rightarrow Fe_3O_4 + 2TEA + 4H_2O. \quad (2)$$

Figure 1b shows a typical current transient for deposition voltage of −1.1 V, which is very close to the reduction peak. The observed deposition current is about −4 mA/cm^2, as expected from the polarization curve for the elected working electrode potential.

Figure 2 is SEM images of electrodeposit obtained at −1.1 V and deposition time of 40 min. The growth of a non-compact layer with large and flat blocks formed by granular aggregates is clearly seen. A typical morphology that was observed for samples prepared with the same potential and different deposition times. EDS measurements at low magnifications (×1,000 to ×5,000) at various regions of the surface, allowed the measurement of a Fe/O atomic percent ratio within 0.65 and 0.85. For magnetite, Fe_3O_4, the ratio is equal to 0.75, indicating that the deposits are non-homogeneously formed with deviations in stoichiometry. Despite of the porous appearance of the deposit, a thickness of about 200 μm was estimated from SEM cross-section measurements, corresponding to a deposition rate of 5 μm/min.

Figure 3 shows normalized hysteresis curves obtained by applying the magnetic field parallel and perpendicular to

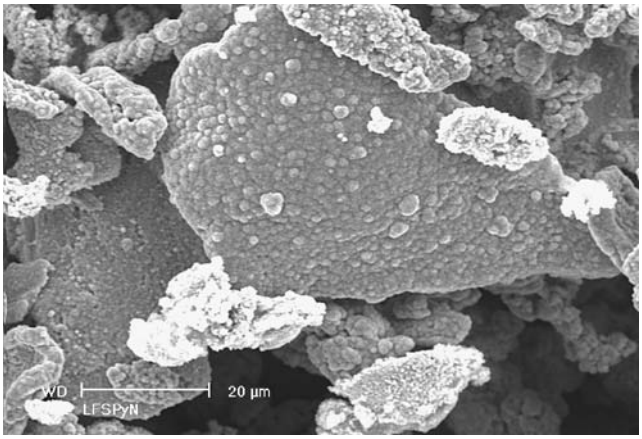

Fig. 2 SEM micrograph of the iron oxide electrodeposit obtained on Cu substrates at −1.1 V

the surface of the electrodeposits. The magnitude of the coercive field is of about 80 Oe, and the parallel curve shows a higher squareness which is consistent with the planar morphology of the deposits.

Figure 4 is a parallel magnetoresistance curve of a sample with an electrical resistance (R) of 712 Ohm at zero magnetic field. A negative MR effect of −6.2% was measured with a reduced hysteresis loop, i.e., low coercivity. The MR hysteresis appears at magnetic fields close to the coercivity (80 Oe) of the electrodeposited layers, as typically observed in systems with giant magnetoresistive (GMR) response [12]. Perpendicular magnetoresistance was also measured (results not shown), and a negative MR effect of −5% was obtained, indicating the simultaneous presence of anisotropic magnetoresistance (AMR). Additionally, no MR saturation was observed in the range of variation of the applied magnetic field (−3 to 3 kOe). The MR curve shown in Fig. 4 was obtained with an applied current of 100 µA.

It is interesting that the longitudinal MR is larger than the transversal one. In 3d alloys, this would have been the opposite because the MR is composed of the GMR plus the AMR parts. The GMR part should be the same for transversal and longitudinal; however, the transversal AMR has the same sign that the GMR, while the longitudinal AMR has opposite sign of the GMR [18]. Then, it is clear that the transversal component of the MR should be larger than the longitudinal component. In our case, we do not have a 3d alloy but an oxide with a band structure much different, and then the rule of the 3d alloys may not be applicable. In fact, what all our experiments show is that for the oxide-like magnetite that we have grown, the transversal AMR has opposite sign to the GMR and the longitudinal the same sign as the GMR. This is just the opposite in the case of the 3d alloys. In semiconductors, for example, the AMR can be one sign or the other depending on the doping [19]. This is just a question of the resistivity tensor [20]. Similar effects have been seen in crystalline and film magnetite [1, 21].

In order to investigate the dependence of the MR effect as a function of the applied current, a sample with R=80 Ω was submitted to measuring currents varying in the range from a few microamps to tens of milliamps. Figure 5a shows a slow decrease of the MR effect with the increase of the magnitude of the electrical current, for currents as high as 10 mA. The rapid decrease for currents above 10 mA is certainly related to the current versus voltage curve

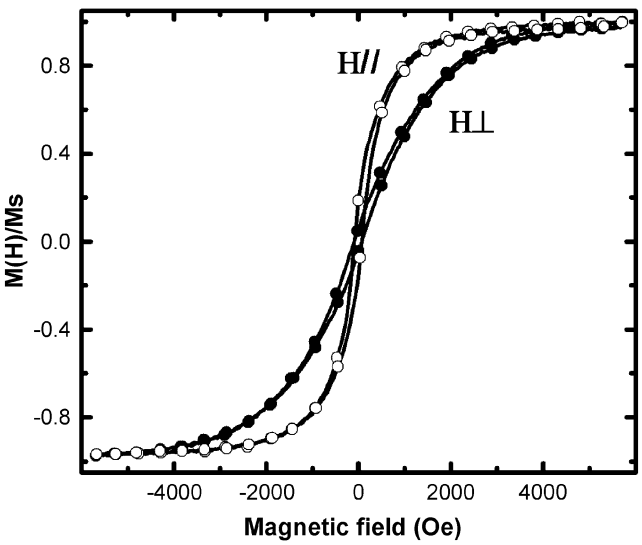

Fig. 3 Normalized magnetization curves measured with the magnetic field applied parallel (//) and perpendicular (⊥) to the sample surface

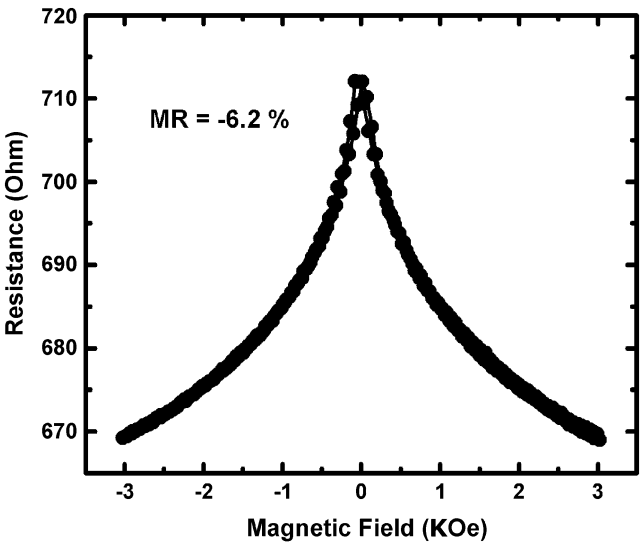

Fig. 4 Magnetoresistance measurement of an electrodeposit with an electrical resistance at zero magnetic field of 712 Ohm

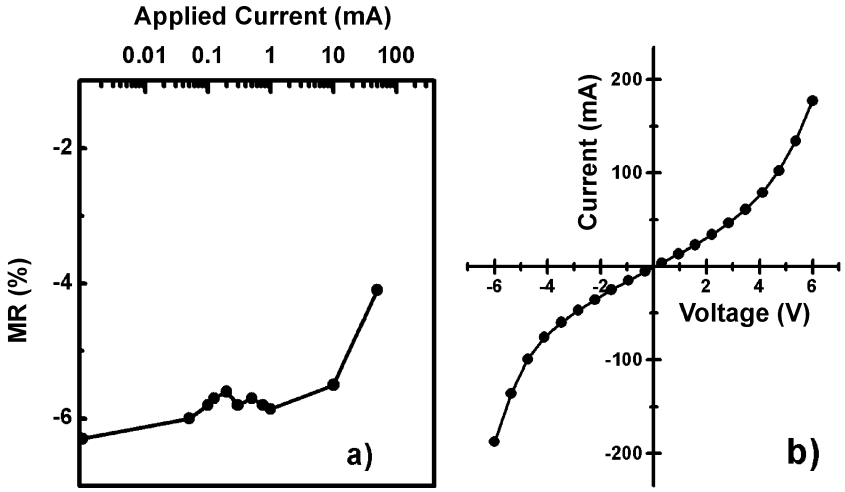

Fig. 5 **a** MR effect as a function of the measuring current and **b** current versus voltage curve characteristic of tunneling through a barrier

displayed in Fig. 5b. This curve shows the common feature of a transport mechanism based on the tunneling of carriers through a barrier. Preliminary measurements of the resistance as a function of the temperature displayed a linear relationship in Log R vs. $T^{-1/2}$ plots, corroborating with the observed tunneling mechanism for the electrical conductance of the device (results not shown). In our samples, the magnetotransport should occur through tunneling at intergranular barriers as could be inferred from SEM images (Fig. 2). Tunneling mechanism through barriers at grain boundaries have been observed in magnetite compacted powders [12], nanoparticles systems [15, 16], and polycrystalline thin films [1], for example.

Figure 6 is a measurement of the magnetoresistance as a function of time with the field being cycled from −3 to 3 kOe at a rate of 2 Oe/s, for an applied current of 0.1 mA.

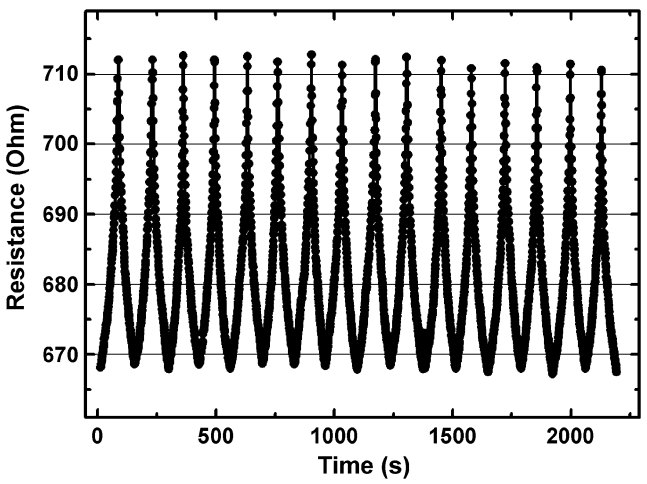

Fig. 6 Cycled measurements of the magnetoresistance of sample showed in Fig. 4 for magnetic field varying in the interval between −3 to 3 kOe

In this case, eight cycles were applied and a small drift was observed, which was further reduced by cycling for longer times.

The results shown above are adequate for the development of magnetic sensors, when considering the magnitude of the MR effect, the reduced hysteresis and the temporal stability. The magnitude of the electrical resistance of the devices can be adjusted by varying the thickness and the area of the electrodeposits. Resistivities of 2–6 kΩ cm were obtained by taking into account the geometry of the electrodeposited samples. Due to the porous nature of the deposits, these values are much higher than the ones reported by Kitamoto et al. [7] of 2–200 Ω cm and 5 orders of magnitude higher than the bulk value of 10 mΩ cm for magnetite. However, high resistivities are adequate for practical devices, since it results in the appearance of high voltage values for low applied currents, and consequently, high magnetovoltage responses easily to be measured. In our devices, magnetovoltages of tenths of Volt were observed.

Conclusion

Deposits of iron oxide with composition close to magnetite phase were obtained by electrodeposition on PCB substrates. The morphological analysis shows non-compact layers with large and flat blocks formed by granular aggregates. A parallel magnetoresistive effect of −6.2% was observed at room temperature for magnetic field with intensity varying in the range of 0 to 3 kOe. The magnetoresistive response of the layers is stable, without saturation with the increase of the magnetic field and hysteresis for very low magnetic field intensities, a performance that is adequate for the development of magnetic sensors.

Acknowledgements The present research was supported by FAPESC, CNPQ and CAPES (Brazil), CICyT (Spain) and MUNDIS project (EC). The authors wish to thank M. F. Alamini and D. Aragão for helping with the preparation of the electrodeposited layers at the LFFS/UFSC. RGD is currently receiving a post-doc stipend from CNPQ. JSC present address is Facultad de Quimica/Materiales, Universidad Autónoma de Querétaro, México.

References

1. Lui H, Jiang EY, Bai HL, Zheng RK, Wei HL, Zhang XX (2003) Appl Phys Lett 83:3531 doi:10.1063/1.1622440
2. Hong JP, Lee SB, Jung YW, Lee JH, Yoon KS, Kim KW et al (2003) Appl Phys Lett 83:1590 doi:10.1063/1.1604466
3. Mi WB, Shen JJ, Jiang EY, Bai HL (2007) Acta Mater 55:1919 doi:10.1016/j.actamat.2006.10.050
4. Eerenstein W, Palstra TTM, Saxena SS, Hibma T (2002) Phys Rev Lett 88:2472041 doi:10.1103/PhysRevLett.88.247204
5. Ogale SB, Ghosh K, Sharma RP, Greene RL, Ramesh R, Venkatesan T (1998) Phys Rev B 57:7823 doi:10.1103/PhysRevB.57.7823
6. Bohra M, Venkataramani N, Prasad S, Kumar N, Misra DS, Sahoo SC et al (2007) J Magn Magn Mater 310:2242 doi:10.1016/j.jmmm. 2006.10.822
7. Kitamoto Y, Nakayama Y, Abe M (2000) J Appl Phys 87:7130 doi:10.1063/1.372953
8. Nishimura K, Kohara Y, Kitamoto Y, Abe M (2000) J Appl Phys 87:7127 doi:10.1063/1.372952
9. Terrier C, Abid M, Arm C, Serrano-Guisan S, Gravier L, Ansermet J-P (2005) J Appl Phys 98:086102 doi:10.1063/1.2099534
10. Kothari HM, Kulp EA, Limmer SJ, Poizot P, Bohannan EW, Switzer JA (2006) J Mater Res 21:293 doi:10.1557/jmr.2006.0030
11. Coey JMD, Chien CL (2003) MRS Bull 28:720
12. Coey JMD, Berkowitz AE, Balcells LL, Putris FF, Parker FT (1998) Appl Phys Lett 72:734 doi:10.1063/1.120859
13. Margulies DT, Parker FT, Rudee ML, Spada FE, Chapman JN, Aitchison PR et al (1997) Phys Rev Lett 79:5162 doi:10.1103/PhysRevLett.79.5162
14. Hibma T, Voogt FC, Niesen L, van der Heijden PAA, de Jonge WJM, Donkers JJTM et al (1999) J Appl Phys 85:5291 doi:10.1063/1.369857
15. Zeng H, Black CT, Sandstrom RL, Rice PM, Murray CB, Sun S (2006) Phys Rev B 73:020402 doi:10.1103/PhysRevB.73.020402
16. Wang W, Yu M, Batzill M, He J, Diebold U, Tang J (2006) Phys Rev B 73:124412
17. Lu ZL, Xu MX, Zou WQ, Wang S, Liu XC, Lin YB et al (2007) Appl Phys Lett 91:102508 doi:10.1063/1.2783191
18. McGuire TR, Potter RI (1975) IEEE Trans Magn 11:1018 doi:10.1109/TMAG.1975.1058782
19. Lehmann HW (1967) Phys Rev 163:488 doi:10.1103/PhysRev.163.488
20. Chikazumi S (1997) Physics of ferromagnetism, 2nd edn. Oxford Science publications, New York
21. Ziese M, Blythe HJ (2000) J Phys Condens Matter 12:13 doi:10.1088/0953–8984/12/1/302